SRM Design Based on the Sequence Subspace Multi-objective Optimization

Ma Hongbo, Li Hongmei *, Liu Liwen, Ma mingna and Chen Zhiwei
Department of Electrical Engineering, Hefei University of Technology, Hefei, China
Email: hongmei.li@hfut.edu.cn

***Abstract* — For an optimal design of synchronous reluctance motor (SRM), rotor topology and the choice of numerous design variables remain a significant challenge. Generally, the rotor of SRM is only designed in the axial or radial direction, and the design variables are reduced based on experience; however, the above process is time-consuming. In this paper by comparing performances of SRM with different pole/slot combinations and the numbers of flux barriers, the SRM topology with 4-poles/36-slots combinations, distributed windings, and three-layer flux barrier is first proposed. And then, the step-skewed rotor with asymmetry flux barriers and flat tips are adopted. Further, the Taguchi method, differential evolution (DE) algorithm and Pareto evaluation are integrated to implement the sequence subspace multi-objective optimization, the proposed SRM design scheme is obtained. Finally, a 3kW SRM prototype is designed and its FEA (finite element analysis) is carried out to validate the technical advantages of proposed SRM topology and design methods.**

***Index Terms* – SRM, Step-skewed rotor, Asymmetry flux barriers, Taguchi method, Sequence subspace multi-objective optimization.**

I. INTRODUCTION

Recently, due to the price fluctuation of permanent magnets (PM) and the instability of the supply of PM materials, the synchronous reluctance motor (SRM) has become increasingly attractive in various fields, especially in electric vehicles and industrial applications. The SRM has good flux-weakening performance and structural stability to avoid the use of PM. However, it still has some disadvantages such as large torque ripple, low torque density and low power factor, which restricts its popularization and application.

To reduce the torque ripple of SRM, the common solutions are summarized as follows. The step-skewed rotor is adopted, and the best step-skewed way and angle are studied [1]. The Machaon type flux barrier is proposed to eliminate a certain number of air-gap MMF harmonics [2]. The optimal flux-barrier tip [3] and right-left asymmetric flux-barrier can achieve lower torque ripple without reducing output torque [4]. The multi-layer windings and optimization of coil turns is presented [5], etc. The researches on the improvement of SRM torque density mostly start with the rotor topology optimization. By adding external rotor sleeve, the rotor magnetic bridge and the center support part are cancelled to reduce the q-axis inductance [6], fractional-slot concentrated windings and novel rotor can increase the saliency ratios [7]. In view of the low power factor, the key parameters of SRM are optimized [8], or dual-phase materials are used [9].

As for the multi-objective optimization of SRM, generally all the structural parameters of the rotor are used as the optimization parameters [10], however, it is time-consuming. Therefore, the benefit of multi-objective optimization is effectively improved by Taguchi method or setting restriction [11-12]. The trade-off idea are put forward to balance the multi-objective optimization benefits and the calculation cost, and the differential evolution algorithm (DE) has the advantage of good optimization effect and rapid convergence [13].

For the SRM, on the one hand, the rotor topology and design variables should be properly chosen. On the other hand, the optimization benefits can be improved by the appropriate optimization method. Therefore, in this paper, the SRM topology and objectives of optimization are firstly presented. And then, the Taguchi method is proposed to determine the optimized variables and implement the subspace division after setting the restriction. Furthermore, the sequence subspace multi-objective optimization is implemented based on the finite element analysis (FEA) to verify the analysis results of SRM design.

II. DETERMINATION OF SRM TOPOLOGY

For SRM motor, the average toque decreases with the increase of the pole numbers, and it remains almost constant when employing different stator slot numbers but with the same pole number. In addition, the torque ripple decreases significantly as the stator slot number increases [14]. By comparing the torque ripple of 4poles/12slots, 4poles/24slots and 4poles/36slots SRM, the 4poles/36slots SRM with lowest torque ripple is selected. The three or four layers flux-barrier has the highest torque density and lowest torque ripple. After considering the complexity of the flux-barrier and the stability of the rotor structure, the rotor with three layers flux-barrier is adopted. Furthermore, the distributed windings are adopted to reduce the torque ripple and iron loss.

The torque ripple of SRM is large since the uneven rotor magnetic resistance and large air gap harmonics. In order to reduce large torque ripple, [1] and [4] propose the improvement method in axial or radial direction, respectively.

The harmonics of tooth and air gap can be weakened by changing the relative position between the rotor and stator. The principle of step-skewed rotor is the same as that of skew-slot stator. The step-skewed coefficient corresponding to the v order harmonics is

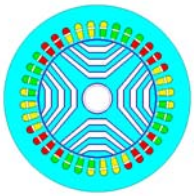

Fig. 1(a) SRM Topology

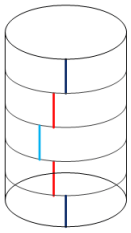

Fig. 1(b) Rotor Topology

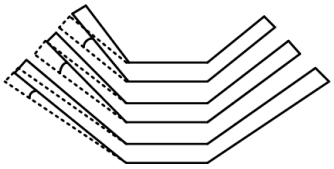

Fig. 1 (c) Asymmetry Flux-barrier
Fig. 1 Proposed SRM Topology

$$k_{skew\_pole} = \frac{\sin[\frac{n\forall\alpha}{2(n-1)}]}{n*\sin[\frac{\forall\alpha}{2(n-1)}]} \qquad (1)$$

where α is electric angle of the step-skewed rotor and n is axial segment number.

The $\left(\frac{\mathrm{LCM(z,2p)}}{\mathrm{p}} \pm 1\right)$ order harmonics of tooth and the $\frac{\mathrm{LCM\ (z,2p)}}{p}$ order harmonics of air gap can be weakened by the step-skewed method, and the coefficient of the corresponding order harmonics is set to zero.

$$\frac{n\frac{\mathrm{LCM(z,2p)}}{p}\alpha}{2(n-1)} = \pi \qquad (2)$$

Then the electric angle of the step-skewed rotor can be obtained and given as

$$\alpha = \frac{2p\pi}{\mathrm{LCM(z,2p)}}\frac{n-1}{n} \qquad (3)$$

where p is the number of pole-pairs, z is the number of slots, and LCM(z,2p) is the least common multiple of the number of slots and the number of poles.

When the step-skewed rotor is used, the more number of rotor segments, the better performance. However, in actual manufacture, the more number of rotor segments, the higher cost. Hence, considering the harmonic of tooth and air gap, the five segments arranged in v-shaped skew orders is used and the step-skewed angle is set as the design variable.

The torque ripple increases due to the discontinuous change of magnetoresistance, because the three layers of flux-barrier is encountered and separated with the stator tooth at the same time. Therefore, the left-right asymmetric structure is proposed to reduce the torque ripple without sacrificing the torque density. Then, the 1/4 model is established and consuming time of FEA can be reduced. Considering the barrier tips is important to the mechanical properties of SRM. According to the contrast of different shape of barrier tips in [15], the flat barrier tips are chosen to reduce the mechanical stress and make it distribute more uniformly. To this end, the proposed topology of SRM in Fig. 1(a) shows that the rotor adopts a three layer magnetic barrier structure with the step-skewed rotor, as shown in Fig. 1(b). The asymmetry flux-barrier is shown in Fig. 1 (c).

In this paper, the SRM torque performance of symmetric structure, step-skewed structure, left-right asymmetric structure, step-skewed and left-right asymmetric structure are compared in Fig. 2. It is clear that the proposed SRM topology can reduce the torque ripple and guarantee the torque density.

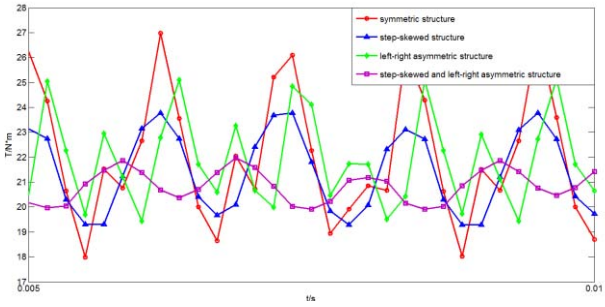

Fig. 2 The Torque Performance Comparison of Different structure SRM

III. THE MULTI-OBJECTIVE OPTIMIZATION OF SRM

A. *The simplifying of SRM rotor topology*

SRM has complex rotor structure, and how to find the optimization variables from many rotor design variables is a hot issue. The rotor topology is first simplified to reduce the number of design variables and the implementation is given as follows:

(1) The length and width of horizontal flux-barrier, width of flux path and the difference of opening angle is set to the same value in each layer, so that the flux is uniformly distributed in the rotor and local magnetic saturation is avoided to reduce iron loss;

(2) The thickness of the magnetic ribs is inversely proportional to the electromagnetic performance and is proportional to the mechanical properties. In consideration of the processing and stress, the thickness of each magnetic rib is set to the same value and the smaller the better;

(3) To make the mechanical stress distribution more uniform, the length of barrier tips is set to the same value. Because the chamfer radius and the angle of the flat barrier tips have little effects on the electromagnetic performance and have a great influence on the mechanical properties, so it is put into the optimization of the mechanical performance.

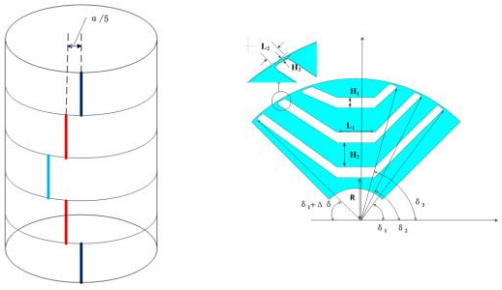

Fig. 3 The Simplified SRM and its design Variables

The simplified SRM topology is shown in Fig.3 and its design variables are: the angle of the step-skewed rotor

α, the length of horizontal section L_1, the width of horizontal flux-barrier H_1, the width of flux path H_2, opening angle of each layer flux-barrier δ_1, δ_2, δ_3, the length of magnetic rib L_2, the thickness of the magnetic rib H_3, the distance between the magnetic barrier and the axis R, and the asymmetry angle of flux-barrier $\Delta\delta$.

B. Determination of Optimization Objectives

Considering the disadvantages of large torque ripple, low torque density and low power factor of SRM, the average torque, torque ripple and power factor are selected as the objective functions and the torque ripple is calculated by

$$T_R = T_{Max} - T_{Min} \tag{4}$$

where T_{Max} and T_{Min} denote the maximum and minimum torque values, respectively.

C. Sequential Subspace Multi-objective Optimization of SRM

The simplified SRM still has 11 design variables. Therefore, the Taguchi method is introduced to determine the motor optimization variables. Take the other four equal different adjacent values as factors and the specific value is shown in Table I. The orthogonal test of L^{50} (5^{11}) shown in Table II is set at 5 levels of 11 variables, which L is the orthogonal table code, 50 is the number of experiments, 11 is the number of design variables, and 5 is the level number of variables.

TABLE I
EACH LEVEL OF DESIGN VARIABLES

Variables	Level 1	Level 2	Level 3	Level 4	Level 5
H_1 (mm)	3	3.5	4	4.5	5
H_2 (mm)	3	3.5	4	4.5	5
L_1 (mm)	10	12	14	16	18
R (mm)	16	17.5	19	20.5	22
L_2 (mm)	3	3.75	4.5	5.25	6
δ_1 (deg)	50	51	52	53	54
δ_2 (deg)	62	63	64	65	66
δ_3 (deg)	73	74	75	76	77
$\Delta\delta$ (deg)	0	1.25	2.5	3.75	5
H_3 (mm)	0.5	0.625	0.75	0.875	1
α (deg)	0	2.5	5	7.5	10

The influence weight of design variables on objective function are given as

$$\mathrm{T} = \sum_{i=1}^{n} y_i \tag{5}$$

$$S_j = \frac{1}{t}\sum_{i=1}^{m} S_{ji}^2 - \frac{1}{n}T^2 \tag{6}$$

where m is the levels of each variables, n is the number of experiments, and t is the number of experiments of variable j per level. y_i denote the No. i experiment result of each variable, and S_{jm} means the sum of the quality characteristics of m level of variable j.

The influence weight of each design variables is obtained through calculation in Table III, then the optimization variables are obtained and shown as R, H_1, H_2, H_3, L_2, δ_1, δ_3, $\Delta\delta$. And then, the optimization space is divided into three subspaces as shown in Table IV. In each subspace, the differential evolution algorithm and Pareto evaluation are integrated to implement the multi-objective optimization based on the finite element model of SRM.

TABLE II
EXPERIMENTAL PLAN OF L^{50} (5^{11})

Num	H_1	H_2	L_1	R	L_2	δ_1	δ_2	δ_3	$\Delta\delta$	H_3	α
1	1	1	1	4	1	1	1	2	2	4	3
2	1	2	2	3	5	4	5	1	5	5	5
3	1	3	3	2	4	2	3	5	1	2	4
4	1	4	5	5	3	3	2	4	4	3	1
5	1	5	4	1	2	5	4	3	3	1	2
6	2	1	2	5	4	5	5	5	4	1	3
						……					
45	4	5	5	2	2	2	5	4	5	4	3
46	5	1	1	3	4	2	2	4	2	5	2
47	5	2	2	2	3	3	4	3	3	2	3
48	5	3	3	5	2	5	1	2	5	3	5
49	5	4	5	1	1	1	5	1	1	1	4
50	5	5	4	4	5	4	3	5	4	4	1

TABLE III
IMPACT WEIGHT OF EACH DESIGN VARIABLES

Variable	Impact weight on Average Torque	Impact weight on Torque Ripple	Impact weight on Power Factor
H_1	5.93%	10.72%	17.59%
H_2	15.13%	3.66%	6.27%
L_1	0.65%	2.38%	0.24%
R	63.7%	15.18%	37.28%
L_2	2.31%	7.79%	12.91%
δ_1	0.92%	26.27%	1.44%
δ_2	4.28%	2.58%	4.81%
δ_3	2.19%	9.91%	1.84%
$\Delta\delta$	0.56%	11.68%	1.98%
H_3	3.58%	5.4%	15.5%
α	0.75%	4.43%	0.14%

TABLE I
SUBSPACE DIVISION

Subspace	Optimization Variables
Highly-Significant Subspace (S_1)	R, H_1, H_2
Significant Subspace (S_2)	H_3, L_2
Non-Significant Subspace (S_3)	δ_1, δ_3, $\Delta\delta$

The effects of SRM sequence subspace optimization are shown in Table V. It is clear that the simultaneous optimization of proposed SRM is obtained. The number of motor optimization variables is reduced from 8 to 2 or 3 in each optimized subspace, so the speed of convergence has been improved.

TABLE II
COMPARISON RESULTS OF PRE-OPTIMIZED AND OPTIMIZED MOTOR

	Pre-optimized motor	S_1 optimized motor	S_2 optimized motor	S_3 optimized motor
T_{avg} [N*m]	20.6945	20.8563	21.2803	21.4490
T_R [N·m]	3.9895	1.5285	1.6677	1.5090
PF	0.7762	0.7765	0.7856	0.7987

IV. SRM PROTOTYPE TESTING

In order to achieve high torque density and power factor, it is necessary to enhance the saliency ratios of SRM, which leads to the thinning of the ribs and the risk of the structural stability. Therefore, the mechanical stress of the ribs must be calibrated. Based on the acquired SRM electromagnetic scheme through sequential subspace multi-objective optimization of SRM, the linear and flat barrier tips is compared, and the angle and radius of barrier tips are adjusted. The mechanical stress is checked at the condition with 150℃ and 5000rpm, the stress and deformation analysis contour plot is provided in Fig.3. It is clear that the flat magnetic barrier structure proposed in this paper can effectively reduce the maximum stress, and make the stress distribution more uniform. Moreover, it meets the mechanical performance requirements at high speed.

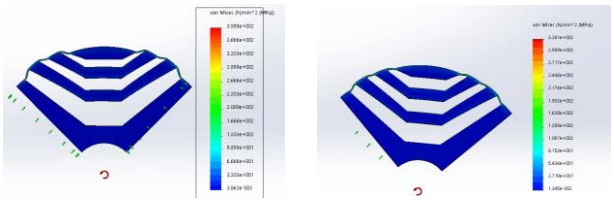

Fig. 3 Stress and deformation contour plot

V. CONCLUSION

To improve characteristics of large torque ripple, low torque density and low power factor of SRM, this paper firstly proposes an appropriate SRM topology. And then, the SRM design is accomplished by combining Taguchi method, DE algorithm and Pareto evaluation to realize the sequence subspace multi-objective optimization. The FEA of a 3kW prototype confirms that the proposed SRM topology and design scheme can meet the multi-target design requirements, which also has the value of design reference and applications.

ACKNOWLEDGMENT

The work was supported by the Natural Science Foundation of China (No. 51377041 and No. 51507043).

REFERENCE

[1] Blum J, Merwerth J, Herzog H G, “Investigation of the segment order in step-skewed synchronous machines on noise and vibration”, Electric Drives Production Conference. IEEE, 2014:1-6.

[2] Bianchi N, Bolognani S, Bon D, et al, “Rotor flux-barrier design for torque ripple reduction in synchronous reluctance motors”, Industry Applications Conference, 2006. Ias Meeting. Conference Record of the IEEE, 2006:1193-1200.

[3] Howard E, Kamper M J, Gerber S, “Asymmetric Flux Barrier and Skew Design Optimization of Reluctance Synchronous Machines”, IEEE Transactions on Industry Applications, 2015, 51(5):3751-3760.

[4] Martinez J, Krischan K, Muetze A, “Minimization of a SynRel’s oscillating torque by calculation of the appropriate skew angle”, Compel International Journal for Computation & Mathematics in Electrical & Electronic Engineering, 2017, 36(3): 824-835.

[5] Kabir M A, Husain I, “New multilayer winding configuration for distributed MMF in AC machines with shorter end-turn length”, Power and Energy Society General Meeting. IEEE, 2016:1-5.

[6] Reddy, Patel Bhageerath, K. Grace, and A. El-Refaie, “Conceptual design of sleeve rotor synchronous reluctance motor for traction applications”, Electric Machines & Drives Conference IEEE, 2016:195-201.

[7] Spargo, Christopher M., et al, “Application of Fractional-Slot Concentrated Windings to Synchronous Reluctance Motors”, IEEE Transactions on Industry Applications 51.2(2015):1446-1455.

[8] Langue L N, Friedrich G, Vivier S, et al, “Optimization of synchronous reluctance machines for high power factor”, Xxii International Conference on Electrical Machines. IEEE, 2016:1976-1982.

[9] Reddy P B, El-Refaie A, Galioto S, et al. “Design of synchronous reluctance motor utilizing dual-phase material for traction applications”, Energy Conversion Congress and Exposition. IEEE, 2015:4812-4819.

[10] Cupertino, Francesco, G. Pellegrino, and C. Gerada. “Design of synchronous reluctance machines with multi-objective optimization algorithms”, IEEE Energy Conversion Congress and Exposition IEEE, 2014:1858-1865.

[11] Azizi, Hossein, and A. Vahedi. “Sensitivity analysis and optimum design for the stator of synchronous reluctance machines using the coupled finite element and Taguchi methods”, Turkish Journal of Electrical Engineering & Computer Sciences 23.1(2015):38-51.

[12] Pellegrino, G, F. Cupertino, and C. Gerada. “Automatic Design of Synchronous Reluctance Motors Focusing on Barrier Shape Optimization”, Industry Applications IEEE Transactions on IEEE 51.2(2015):1465-1474.

[13] Cupertino, Francesco, G. Pellegrino, and C. Gerada. “Design of synchronous reluctance machines with multi-objective optimization algorithms”, IEEE Energy Conversion Congress and Exposition, 2014:1858-1865.

[14] Wang K, Zhu Z Q, Ombach G, et al. “Optimal slot/pole and flux-barrier layer number combinations for synchronous reluctance machines”, International Conference and Exhibition on Ecological Vehicles and Renewable Energies, 2013:1-8.

[15] Nardo, M. Di, et al. “End barrier shape optimizations and sensitivity analysis of synchronous reluctance machines”, Industrial Electronics Society, IECON 2015 -, Conference of the IEEE, 2016:002914-002919.